Journal of the Brazilian Society of Mechanical Sciences and Engineering (2022) 44:91
https://doi.org/10.1007/s40430-022-03359-4

TECHNICAL PAPER

Development of a hybrid solar thermal power plant with new collector field, and its thermal and exergy analyses

Elahe Javadzadeh[1] · Ali Baghernejad[2]

Received: 4 May 2021 / Accepted: 30 December 2021 / Published online: 21 February 2022

Abstract

In the present study, a hybrid solar thermal power plant (STPP) developed with a new LS-3 collector is introduced and analyzed by the exergy analysis. The results are compared with a hybrid STPP in the base case. Energy and exergy analyses are also carried out to understand the performance of the solar fields. In the developed system design, a new parabolic trough collector field is added to increase the temperature of generated steam entering the steam turbine. The analysis of results for the solar fields shows that the energy and exergy losses in the collector–receiver subsystem of the Therminol VP-1 oil collector field are more than the other subsystems. The maximum exergy destruction of the system occurs in the auxiliary boiler and then in the solar collectors' fields. Also, comparative results of the newly developed system with the base case show that exergy destruction decreases from 6.61 MW to 3.1 MW, and exergy efficiency increases from 7% to 11.97% for developed STPP with LS-3 collectors and STPP in the form of the base case, respectively.

Keywords Exergy · Parabolic trough collector · Solar energy · Solar thermal power plant

List of symbols

A	Area (m^2)
C_p	Specific heat (kJ/kg K)
e	Specific exergy (kJ/kg)
$\dot{E}$	Exergy rate (MW)
e_k^{ch}	Standard chemical exergy rate of kth component
H	Specific enthalpy (kJ/kg)
IR	Irreversibility (MW)
I	Solar intensity (W/m^2)
K	Thermal conductivity (W/mK)
L	Length (m)
$\dot{m}$	Mass flow rate (kg/sec)
N	Number of collectors
P	Pressure (bar)
$\dot{Q}$	Heat transfer rate (MW)
R	Gas constant (kJ/kg K)
R_b	Geometric factor
s	Specific entropy (kJ/kg K)
T	Temperature (°C)
W	Work (kJ)
$\dot{W}$	Work rate (MW)
W_0	Aperture (m)
x	Molar fraction

Greek symbols

α	Absorptivity of absorber
ε	Exergy efficiency
$\eta_\circ$	Optical efficiency
η	Energy efficiency
θ	Angle of incidence
θ_z	Zenith angle
ρ	Density (m^3/kg)
τ	Transmissivity of cover
ϕ	Ratio of fuel chemical exergy to lower heat value

Subscripts

0	Dead state
a	Ambient
b	Beam
c	Collector
ch	Chemical
D	Destruction
F	Fuel

Technical Editor: Monica Carvalho.

✉ Ali Baghernejad
abaghernezhad@gmail.com

Elahe Javadzadeh
elahe.javadzadeh@gmail.com

[1] Engineering School, West Tehran Islamic Azad University, Tehran, Iran

[2] Mechanical and Aerospace Engineering Department, School of Engineering, Garmsar branch, Islamic Azad University, Garmsar, Iran

f	Fluid
i	Inlet
k	Component
L	Loss
o	Outlet
P	Product
ph	Physical
Q	Heat transfer
r	Receiver
s	Solar/absorber
u	Useful
w	Work

Abbreviations

DE	Dish/engine system
CHP	Combined heat and power
CRS	Central receiver
CSP	Concentrating solar power
CRS	Central receiver system
LF	Linear Fresnel
LHV	Lower heating value (kJ/kg)
LS-3	Luz system three
SLT	Second law of thermodynamics
SRC	Steam Rankine cycle
STPP	Solar thermal power plant
ORC	Organic Rankine cycle
PTC	Parabolic trough collector

1 Introduction

During recent decades, the significant growth of the global energy demand has led to global warming and high consumption of fossil fuels which caused compulsory usage of renewable energy resources to cover the world energy demand and attain sustainable energy in the future. Among different energy resources, solar energy is highly abundant and does not restrict to the geographic region, i.e., it possesses the highest potential compared to other renewable sources. As far as the equipment used in solar thermal power plants, optical concentration devices are essential options for power generation. In the early 80s, the SEGs plants were the first concentrating solar power plants (CSP) established in California's Mojave Desert. The CSP technologies are categorized into four systems: linear Fresnel reflector systems (LF), parabolic trough collectors (PTC), central receiver systems (CRS), and dish/engine systems (DE). For electricity production in CSP plants, first, the concentrators focus sunlight into a receiver. Then, as the working oil temperature increases to a high temperature set-point, this heated oil delivers to a steam turbine connected to the generator. Among the CSP technologies, the most conventional system is PTCs which widely influence the global market of solar plants [1–4].

Exergy analysis is the stem of the second law of thermodynamics (SLT), which effectively enhances energy resource usage efficiency while recognizing the reasons, variety, locations, and values of inefficiencies. The assessment of efficiencies, generally, is performed via the exergy analysis rather than energy analysis. Exergy analysis is often regarded as a measuring criterion to become close to the ideal form of a thermodynamic process. Therefore, using exergy analysis for solar thermal power plants is a powerful tool that helps define the losses and enhance efficiency [5–7].

A significant volume of articles about analyzing parabolic trough collector solar thermal power plants have been published in the last two decades. Different Rankine cycle modifications have been carried out to improve the performance and reduce the fuel consumption of thermal power plants. Kaushik et al. [8] and Singh et al. [9] studied the energy and exergy analyses of a solar thermal power system, including a Rankine cycle with reheating. Their results showed a considerable energy loss in the condenser, whereas the collector–receiver had the highest exergy loss. Wu et al. [10] simulated a dynamic model of a 5 MW solar thermal power plant and performed exergy analysis of the system. They found that the maximum heat and exergy losses occurred in the condenser and solar collector. Moreover, they observed that the thermal efficiency and exergy efficiency increased as system capacity increased. Energy and exergy analyses of parabolic trough solar collectors combined with a double-stage steam turbine in Rankine cycles were studied by Noorpoor et al. [11]. Their results revealed that the maximum exergy destruction occurred in the solar collector, and using the genetic algorithm for optimization process improved the exergy efficiencies by 58.03%. Vakilabadi et al. [12] carried out the dynamic simulation and the second law of thermodynamic analysis for a SEGS VI power plant. They found that the solar collector had the most exergy destruction value and the boiler's fuel consumption and the exergy efficiency were at their maximum values during the nighttime hours.

Also, several researchers studied various configurations of Rankine cycles with different heat transfer fluids for solar thermal power plants from the view of energy and exergy efficiencies. Studying different refrigerants of the organic and steam Rankine cycles combined with parabolic trough solar collectors based on SLT analysis was carried out by Al-Sulaiman [13]. His results showed that the R134a refrigerant had the most impact on the effectiveness of the exergy, while solar irradiation played an essential role in increasing exergy efficiency. Kerme and Orfi [14] analyzed the organic Rankine cycle with parabolic trough solar collectors thermodynamically, estimating eight working oils for the system. They reported that the maximum exergy destruction rate

took place at the parabolic trough solar collector. Moreover, their results showed that by applying high inlet temperature turbine, the electrical efficiency and the net power output enhanced, and the total exergy destruction rate and the turbine size parameter decreased. Singh and Mishra [15] presented exergy and energy analyses integration of supercritical organic Rankine cycle and solar parabolic trough collector utilizing different refrigerants. They demonstrated a connection between solar irradiation intensity and turbine inlet pressure with exergy destruction and efficiency. It was shown that R600a and R152a had the highest exergy efficiency, whereas the toluene and cyclohexane had the most exergy destruction among all the refrigerants. However, 80% of the overall exergy destruction rate took place in the solar collector. Habibi et al. [16] investigated the energy and exergy analyses for three different configurations of steam Rankine cycle-organic Rankine cycle (SRC-ORC) utilizing nanofluid-based parabolic trough solar collector. They observed the configuration that the remaining nanofluid's heat of evaporator steam Rankin cycle was absorbed by the organic Rankine cycle evaporator had higher output power than a simple steam Rankin cycle because of the condensation pressure. Also, for this configuration, due to the higher enthalpy difference of the working fluid, the required collector area increased, and the energy and exergy efficiencies decreased.

Furthermore, the performance of combining solar field to the system or replacing components of a steam cycle with a solar field was conducted in [17–19]. Mohammadi et al. [17] changed the closed feedwater heaters with PTCs and thermal storage to improve the net electricity generation of power plants and use the system during the night hours. After this alteration, electricity production increased without excess fuel consumption. It was obtained that the boiler had the maximum exergy destruction rate after the alteration, and the exergy efficiency decreased since the solar collector had a high amount of losses. Vakilabadi et al. [18] studied integrating a SEGS VI power plant with a heat and water recovery system from the energy and exergy point of view. Their results showed that most of exergy losses corresponded to the solar collector and the boiler. After the combination, the system gained 48% of the total exergy loss. Furthermore, the exergy efficiency increased from 20.37% to 20.84%, and net power generation increased from 33.83 MW to 34.01 MW, and drained wastewater reduced. A transient simulation and thermodynamic analysis of a combined heat and power (CHP) plant was performed by Alrobaian [19]. In his case study, the open feedwater heater and closed feedwater heater were exchanged by evacuated tube collectors and parabolic trough collectors. The results showed that the maximum exergy destruction value occurred in the waste incinerator. Also, the system had a higher energy and exergy efficiency and lower exergy loss and C O_2 emission than the simple system.

Iran has high renewable energy resources among other countries in the Middle East, especially in solar energy. Shiraz solar thermal power plant is one of the plants constructed based on the parabolic trough collectors' technology. Several research works have been carried out on the Shiraz solar thermal power plant [20–24]. Yaghoubi et al. [20] simulated various parts of the oil cycle in the 250 kW Shiraz solar power plant to boost the absorption of energy and develop the system's efficiency by applying the appropriate control philosophy. Azizian et al. [21] presented the Shiraz solar thermal power plant's design, building process, and performance evaluation. The operation test displayed a high temperature for oil and the superheated steam generation by 250 °C and 265 °C, which is close to the design conditions. In order to increase the electricity production to 500 kW for Shiraz solar thermal power plant, an auxiliary boiler is added to the system. Baghernejad and Yaghoubi [22] optimized the hybrid Shiraz solar thermal power plant from the view of thermoeconomics. The objective functions for the system minimize the cost of the system and maximize the exergy efficiency. Results indicated that exergy efficiency of the system increased from 7% to 8.26%, and the unit cost of electricity decreased when the capacity and solar field operation periods of the system increased. Following the Shiraz plant improvements, a new solar field was combined with the solar power plant to increase the production of the superheated steam (294 °C). Thermal design and different configurations for integrating the additional collector to the Shiraz solar power plant with a capacity of 500 kW was studied by Azizian et al. [23]. They reported that the proper arrangement had lower water and fuel consumptions. Following the new system design, Niknia and Yaghoubi [24] investigated Shiraz solar thermal power plant integrated with a new collector and an auxiliary boiler to increase the energy efficiency. They revealed that these changes had some benefits, such as decreasing fuel utilization, environmental pollution, and higher power production.

According to the presented literature review, most of the solar thermal power plants contain one solar collector field. For a solar thermal power plant case study such as Shiraz STPP, the energy and exergy analyses with two different collectors' fields and its effect on the system's performance have not been fully examined yet. Therefore, the aim of the present study is the exergy analysis of the 500 kW hybrid Shiraz solar thermal power plant (STPP) developed with the LS-3 collector. In order to enhance the efficacy of the system, equipment with higher exergy destruction should be determined to reduce the consumed fossil fuel. The thermodynamic modeling of this developed system is performed in the MATLAB software.

2 System description

A 250 kW hybrid solar thermal power plant with the parabolic trough collector was installed successfully and located in Shiraz, the southern city in Iran, adjacent to the Fars combined cycle power plant. A schematic diagram of hybrid STPP with a capacity of 250 kW is shown in Fig. 1.[21]. This STPP contains two cycles, an oil cycle and a steam cycle (conventional Rankine cycle). The oil cycle components are a collector's field, three heat exchangers (E201, E202, and E203), a thermal storage tank, and an oil pump. The oil type used in this cycle is considered Behran. The collector's field consists of 48 parabolic trough collectors, eight parallel loops of 6, and each loop has two rows of 3 collectors, and its direction is north–south. The specification of these collectors is presented in Table 1 [22].

The steam cycle components include heat exchangers, a turbine, a condenser, a deaerator, and pumps. The absorbed oil's heat from the sun transfers to the water in the cycle. The water first enters the E201 (Economizer) and converts to the saturated water and then moves to the E202 (Boiler), becomes saturated steam, and when it enters the E203 (Superheater1), changes to the superheated steam. The generated steam pressure, temperature, and mass flow rate are 21 bar, 250 °C, and 0.673 kg/s, respectively [23]. An auxiliary boiler was integrated into the previous system to develop the electricity generation from 250 kW to 500 kW. Figure 2 shows a schematic diagram of a 500 kW hybrid STPP in the form of the base case [22]. The objective of integrating an auxiliary boiler into the system is to produce more superheated steam to compensate for the scarcity of it and use it during the night or day when the solar radiation is not enough [23].

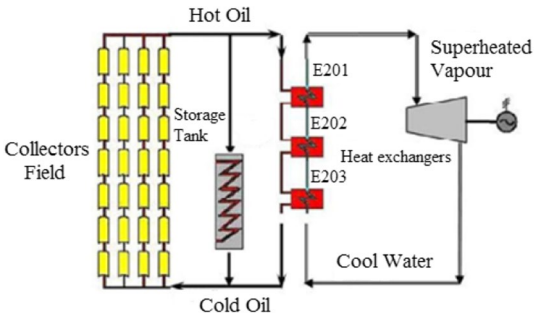

Fig. 1 diagram of hybrid STPP with a capacity of 250 kW [21]

In the new design, a new large size parabolic trough collector in the type of LS-3 was added to the system and considered as an external new oil cycle in the system. Figure 3 shows a schematic diagram of a 500 kW hybrid STPP developed with the LS-3 collector. The Luz system three (LS-3) collector represents the current state-of-the-art in parabolic trough collector design, which would likely be used in the next parabolic trough plant built. The specification of the LS-3 collector is listed in Table 1 [25]. This cycle includes a collector field, oil Therminol VP-1 pump, an oil heat exchanger, and superheater2. Therminol VP-1 is considered as working oil in the new loop. The new collector field supplies 200 kW to the system. The oil heat exchanger component makes a thermal connection by bringing the Therminol VP-1 oil from the LS-3 collector and Behran oil from the primary collectors' field. In this cycle, the collector's inlet temperature is 294 °C, and the outlet temperature increases to 313 °C. Part of the new collector's absorption heat increases the superheated steam's temperature in the superheater2 to 294 °C. The rest of the absorption heat is utilized to heat the outlet oil from the primary collectors' field and produce more saturated steam [26]. The main difference between the first hybrid STPP (see Fig. 1) and the developed hybrid STPP (see Fig. 3) is the generated steam's temperature; generated steam's temperature of the developed system increases by 44 °C. Also, based on the initial designs data, the Behran oil and Therminol Vp-1 are considered as heat transfer fluid for the base case STPP system without LS-3 collector and the developed case STPP system with LS-3

Table 1 Various design parameters of the primary parabolic trough collectors and new collector (LS-3) [22, 25]

Primary collectors specifications			
Length (m)	25	Reflectivity of mirror (ρ)	0.873
Width (m)	3.4	Transmissivity of cover (τ)	0.96
Aperture (m)	3.1	Absorptivity of receiver (α)	0.94
Focal length (cm)	88	Intercept factor (γ)	0.93
New collector specifications (LS-3)			
Length (m)	99	Reflectivity of mirror (ρ)	0.94
Aperture (m)	5.76	Transmissivity of cover (τ)	0.96
Concentration ratio	82	Absorptivity of receiver (α)	0.96
Aperture area per SCA (m^2)	545	Optical efficiency (η_o)	0.8%

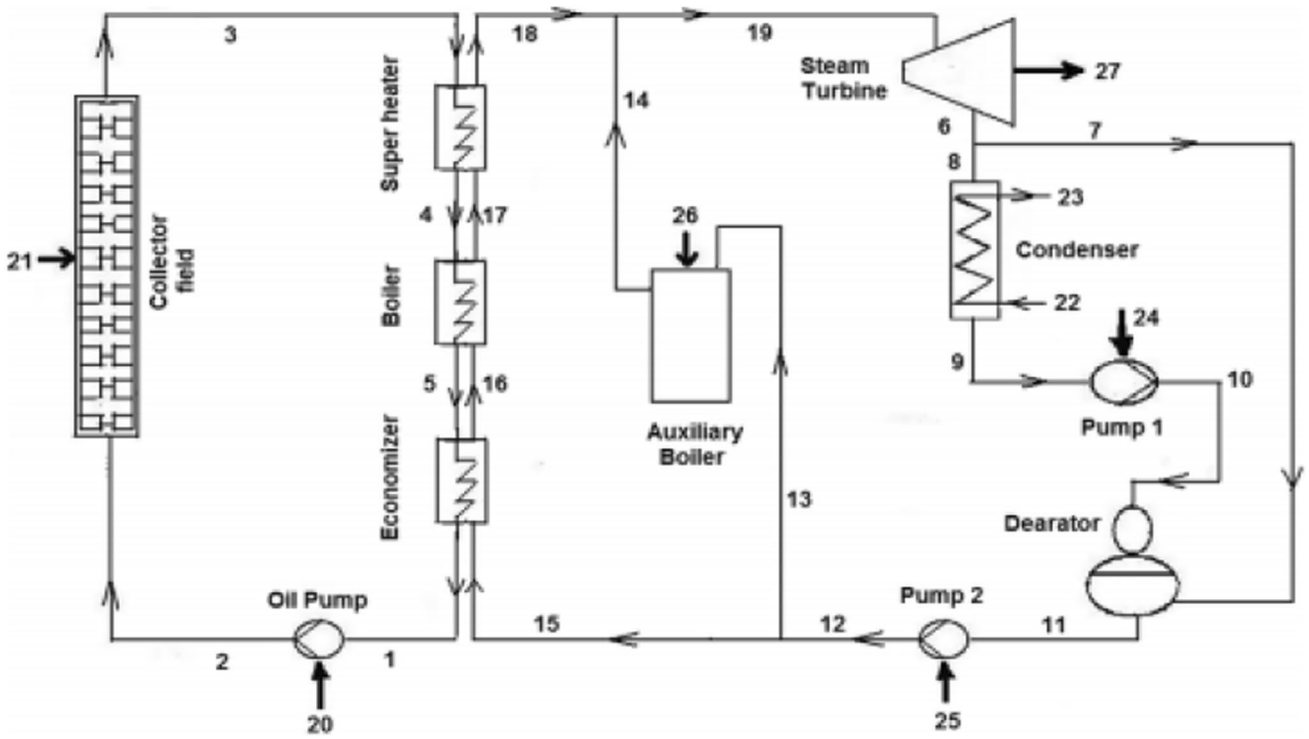

Fig. 2 Schematic diagram of a 500 kW hybrid STPP in the form of the base case [22]

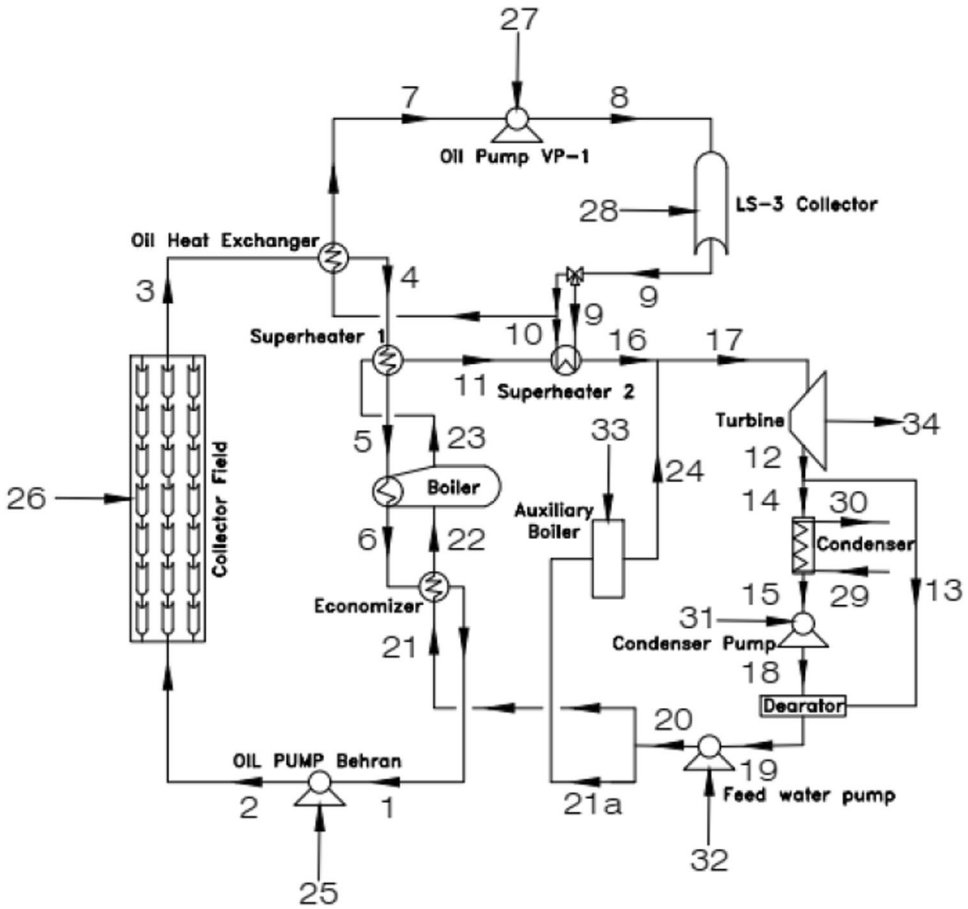

Fig. 3 Schematic diagram of a 500 kW hybrid STPP developed with the LS-3 collector

collector, respectively. In order to get closer to the actual results, the simulation of these systems is carried out based on available design data precisely.

3 Thermodynamic analysis

First and second law analyses have been known as powerful tools for designing and assessment of energy systems. The mathematical modeling of the developed STPP is performed in MATLAB software. The mass, energy, and exergy balance equations are written for each component of oil and steam cycles. The analysis is carried out for Shiraz city on June 21 at 12:00 noon. At this time, the solar intensity at the system site is about 817 $\left(\mathrm{W}/\mathrm{m}^2\right)$. Two various working fluids are carried for oil cycles. The properties of Behran oil are [22]:

$$\begin{aligned} C_P &= 0.8132 - 8.304 \times 10^{-5} \times (T + 273.15) \\ \rho &= 1071.76 - 0.72 \times (T + 273.15) \\ k &= 0.1882 - 8.304 \times 10^{-5} \times (T + 273.15) \end{aligned} \quad (1)$$

The properties of Therminol VP-1 are [24]:

$$\begin{aligned} C_P &= 0.002414 \times T + 5.9591 \times 10^{-6} \times T^2 - 2.9879 \times 10^{-8} \\ &\times T^3 + 4.4172 \times 10^{-11} \times T^4 + 1.498 \\ \rho &= -0.90797 \times T + 0.00078116 \times T^2 - 2.367 \times 10^{-6} \times T^3 + 1083.25 \\ k &= -8.19477 \times 10^{-5} \times T - 1.92257 \times 10^{-7} \times T^2 \\ &+ 2.5034 \times 10^{-11} \times T^3 - 7.2974 \times 10^{-15} \times T^4 + 0.137743 \end{aligned} \quad (2)$$

For the energy and exergy analyses of the system, the following assumptions are considered [27]:

- Ambient temperature and wind speed are 33 °C and 2.5 m/s, respectively.
- A hybrid STPP performs at a steady-state condition.
- The fuel used in the auxiliary boiler is natural gas.
- Heat losses are considered only in the collector fields and ignored in the other components of the system.
- The combustion in the auxiliary boiler is ideal.
- The kinetic and potential energies are neglected due to their very low values compared to the physical and chemical exergies.
- The flow in the pipes is one dimensional.

In the purpose of comparing and evaluating, the combination of the energy and exergy concepts can be considered.

4 Conservation of mass of the system

The general conservation of mass can be written as [6]:

$$\sum_{k=1}^{n} \dot{m}_i = \sum_{k=1}^{n} \dot{m}_o \quad (3)$$

Mass balance equations for the entering and leaving mass flows are applied for each components of the oil and steam cycles and presented in Table 2.

5 Energy analysis

Energy analysis (based on the first law of thermodynamics) is used to understand any process, make design, operation, and control more accessible, identify process improvement opportunities, and allow for eventual optimization [28].

General energy balance equation can be written as [6]:

$$\dot{Q} + \sum \dot{m}_i h_i = \dot{W} + \sum \dot{m}_o h_o \quad (4)$$

Here, $\dot{Q}$ is the rate of net heat input and $\dot{W}$ is the rate of net output work.

The energy efficiency of the system is defined as:

$$\eta = \frac{W_{net}}{Q_h} \quad (5)$$

Here, Q_h is the all energy entering the system through the collector and auxiliary boiler.

Table 2 Components' mass balance equations of a developed STPP

Component	Mass balance equations
Economizer	$\dot{m}_6 + \dot{m}_{21} = \dot{m}_1 + \dot{m}_{22}$
Boiler	$\dot{m}_5 + \dot{m}_{22} = \dot{m}_6 + \dot{m}_{23}$
Superheater 1	$\dot{m}_{23} + \dot{m}_4 = \dot{m}_{11} + \dot{m}_5$
Superheater 2	$\dot{m}_{11} + \dot{m}_9 = \dot{m}_{16} + \dot{m}_{10}$
Oil heat exchanger	$\dot{m}_3 + \dot{m}_{10} = \dot{m}_4 + \dot{m}_7$
Turbine	$\dot{m}_{17} = \dot{m}_{12}$
Auxiliary boiler	$\dot{m}_{21a} + \dot{m}_{33} = \dot{m}_{24}$
Condenser	$\dot{m}_{14} + \dot{m}_{29} = \dot{m}_{15} + \dot{m}_{30}$
Deaerator	$\dot{m}_{18} + \dot{m}_{13} = \dot{m}_{19}$
Oil pump Behran	$\dot{m}_1 = \dot{m}_2$
Oil pump VP-1	$\dot{m}_7 = \dot{m}_8$
Condenser pump	$\dot{m}_{15} = \dot{m}_{18}$
Feedwater pump	$\dot{m}_{19} = \dot{m}_{20}$
Collector	$\dot{m}_2 = \dot{m}_3$
LS-3 Collector	$\dot{m}_8 = \dot{m}_9$

5.1 Solar collectors' field

5.1.1 Parabolic trough collector subsystem

The energy obtained by the parabolic trough collector subsystem is [25]:

$$Q_i = I.N.A = \left(I_b R_b\right) W_0 L \tag{6}$$

where $A = W_0 L$ and $R_b = \frac{COS\theta}{COS\theta_Z}$

Optical efficiency for parabolic trough collectors have a direct relation with optical properties of the collector components and incidence-angle modifier and the relation is:

$$\eta_\circ = K_\theta \left[\rho(\tau\alpha)_n \gamma\right] \tag{7}$$

where $K_\theta = COS\theta - 0.00045656\theta - 0.000040780^2$.

The energy absorbed by the absorber tube can be written as:

$$Q_s = Q_i \eta_0 \tag{8}$$

$$\text{Energy loss} = Q_i - Q_s \tag{9}$$

$$\%\ \text{Energy loss} = \left[\left(Q_i - Q_s\right)/Q_i\right] \times 100 \tag{10}$$

First law efficiency for parabolic trough collector subsystem is defined as:

$$\eta = \frac{Q_s}{Q_i} \tag{11}$$

5.1.2 Receiver subsystem

The useful energy delivered to the working oil in the receiver can be calculated as:

$$Q_u = N.\dot{m}_f.C_{pf}\left(T_{fo} - T_{fi}\right) \tag{12}$$

Or it can be calculated as:

$$Q_u = F_R.Q_s.A_r.U_L\left(T_{fi} - T_a\right) \tag{13}$$

F_R, A_r and U_L are heat removal factors, receiver area and the solar collector overall heat loss coefficient, respectively.

$$\text{Energy loss} = Q_s - Q_u \tag{14}$$

$$\%\ \text{Energy loss} = \left[\left(Q_s - Q_u\right)/Q_s\right] \times 100 \tag{15}$$

First law efficiency for receiver subsystem is defined as:

$$\eta = \frac{Q_u}{Q_s} \tag{16}$$

5.1.3 Collector–receiver subsystem

$$\text{Energy loss} = Q_i - Q_u \tag{17}$$

$$\%\ \text{Energy loss} = \left[\left(Q_i - Q_u\right)/Q_i\right] \times 100 \tag{18}$$

First law efficiency of the collector–receiver subsystem is:

$$\eta = \frac{Q_u}{Q_i} \tag{19}$$

5.2 Oil and steam cycles' components

In the developed STPP (see Fig. 3), the heat from heated oil is given to the steam cycle. Table 3 shows the energy balance equations for all components of oil and steam cycles to calculate the properties of water and oil in the system. The steam turbine's output power is 500 kW and inlet steam temperature and pressure to steam turbine are 294 °C, and 21 bar, respectively. Isentropic efficiency of the steam turbine, condenser pump, feedwater pump, Behran oil pump and VP-1 oil pump are considered 0.65, 0.6, 0.65, 0.55, and 0.65, respectively [22]. Inlet and outlet oil temperatures of the collectors are 221 °C, 265 °C, and for LS-3 collector fields 294 °C, and 313 °C are considered, respectively. The energy balance equations calculate the temperature and enthalpy of superheaters, oil heat exchanger, boiler, and economizer for the developed STPP system.

6 Exergy analysis

Exergy is the useful amount of work from the given quantity of energy at the defined state. Exergy can be categorized into four types: kinetic, potential, physical, and chemical. Physical exergy is the maximum work obtained from the system as the pressure and temperature of it convert to the reference environment's pressure and temperature. Chemical exergy is the maximum amount of work that can be extracted in the situation of reference environment state to the dead state by a process involving heat transfer and exchange of substances [5]. The following relations are the exergy balance, physical exergy and chemical exergy [5, 6]:

$$\dot{E}_Q + \sum_i \dot{m}_i e_i = \sum_o m_o\, e_o + \dot{E}_D + \dot{E}_W \tag{20}$$

$$\dot{E}_Q = \left(1 - \frac{T_\circ}{T_i}\right)\dot{Q}_i \tag{21}$$

$$\dot{E}_W = \dot{W} \tag{22}$$

Table 3 Components' energy balance equations of a developed STPP

Component	Energy balance equations
Economizer	$\dot{m}_{oilpumpbehran}(h_6 - h_1) = \dot{m}_{21}(h_{22} - h_{21})$
Boiler	$\dot{m}_{oilpumpbehran}(h_5 - h_6) = \dot{m}_{22}(h_{23} - h_{22})$
Superheater 1	$\dot{m}_{oilpumpbehran}(h_4 - h_5) = \dot{m}_{11}h_{11} - \dot{m}_{23}h_{23}$
Superheater 2	$\dot{m}_{oilpumpVP-1}(h_9 - h_{10}) = \dot{m}_{11}(h_{16} - h_{11})$
Oil heat exchanger	$\dot{m}_{oilpumpbehran}(h_4 - h_3) = \dot{m}_{oilpumpVP-1}(h_{10} - h_7)$
Turbine	$\eta_t = \frac{h_{17}-h_{12}}{h_{17}-h_{12s}}$, $\dot{W}_{turbine} = 0.5$ MW
Auxiliary boiler	$\dot{m}_{fuel}(LHV\eta_{boiler}) = \dot{m}_{24}h_{24} - \dot{m}_{21a}h_{21a}$
Condenser	$\dot{m}_{cooling}(h_{30} - h_{29}) = (\dot{m}_{water} - \dot{m}_{deaerator})(h_{14} - h_{15})$
Deaerator	$\dot{m}_{deaerator}(h_{13} - h_{19}) = \dot{m}_{water}(h_{19} - h_{18})$
Behran Oil pump	$\dot{W}_{oilpumpbehran} = \dot{m}_{oilpumpbehran}\frac{(W_{oilpumpbehran,\ ideal})}{\eta_{oilpumpbehran}} = \dot{m}_{oilpumpbehran}\frac{(p_2-p_1)}{\rho_1\eta_{oilpumpbehran}}$ $\dot{m}_{oilpumpbehran} = \frac{Q_u}{C_{pbehranoil}(T_3-T_2)}$
VP-1 Oil pump	$\dot{W}_{oilpumpVP-1} = \dot{m}_{oilpumpVP-1}\frac{(W_{oilpumpVP-1,\ ideal})}{\eta_{oilpumpVP-1}} = \dot{m}_{oilpumpVP-1}\frac{(p_8-p_7)}{\rho_7\eta_{oilpumpVP-1}}$
Condenser pump	$\dot{W}_{condenser\ pump} = \dot{m}_{15}\frac{(W_{condenserpump,\ ideal})}{\eta_{condenser\ pump}} = \dot{m}_{15}\frac{(p_{18}-p_{15})}{\rho_{15}\eta_{condenserpump}}$
Feedwater pump	$\dot{W}_{feedwaterpump} = \dot{m}_{19}\frac{(W_{feedwaterpump,\ ideal})}{\eta_{feedwaterpump}} = \dot{m}_{19}\frac{(p_{20}-p_{19})}{\rho_{19}\eta_{feedwaterpump}}$

$$\dot{E} = \dot{E}_{ph} + \dot{E}_{ch} \tag{23}$$

$$\dot{E}_{ph} = \dot{m}\left[(h - h_0) - T_0(s - s_0)\right] \tag{24}$$

$$\dot{E}_{ch} = \dot{m}\left[\sum_{k=1}^{n} x_k e_k^{ch} + RT_\circ \sum_{k=1}^{n} x_k \ln x_k\right] \tag{25}$$

To calculate the chemical exergy of fuel, the following equation can be written as:

$$e_{fuel} = \phi_F \times LHV \tag{26}$$

The LHV is the lower heating value and ϕ is the ratio of fuel chemical exergy to lower heat value. In the auxiliary boiler, chemical exergy is only considered and physical exergy is neglected compared to its chemical exergy due to little amount.

6.1 Solar collectors' field

6.1.1 Parabolic trough collector Subsystem

The exergy received by parabolic through the collector subsystem is [25]:

$$\dot{E}_i = Q_i\left[1 - \left(\frac{T_a}{T_s}\right)\right] \tag{27}$$

The exergy absorbed by the absorber tube can be evaluated as:

$$\dot{E}_c = Q_s\left[1 - \left(\frac{T_a}{T_r}\right)\right] \tag{28}$$

$$\text{Exergy loss} = IR = \dot{E}_i - \dot{E}_c \tag{29}$$

$$\%\ \text{Exergy loss} = \left[(\dot{E}_i - \dot{E}_c)/\dot{E}_c\right] \times 100 \tag{30}$$

Second law efficiency for collector subsystem is expressed as:

$$\varepsilon = \frac{\dot{E}_c}{\dot{E}_i} \tag{31}$$

6.1.2 Receiver subsystem

The useful exergy delivered is:

$$\dot{E}_u = N.\dot{m}_f\left[h_{f0} - h_{fi}\right) - T_a(s_{fo} - s_{fi})] \tag{32}$$

$$\text{Exergy loss} = IR = \dot{E}_c - \dot{E}_u \tag{33}$$

$$\%\ \text{Exergy loss} = \left[(\dot{E}_c - \dot{E}_u)/\dot{E}_u\right] \times 100 \tag{34}$$

Second law efficiency for receiver subsystem is defined as:

$$\varepsilon = \frac{\dot{E}_u}{\dot{E}_c} \tag{35}$$

6.1.3 Collector–receiver subsystem

$$\text{Exergy loss} = \text{IR} = \dot{E}_i - \dot{E}_u \tag{36}$$

$$\%\ \text{Exergy loss} = \left[\left(\dot{E}_i - \dot{E}_u\right)/\dot{E}_u\right] \times 100 \tag{37}$$

Second law efficiency of the collector–receiver subsystem is:

$$\varepsilon = \frac{\dot{E}_u}{\dot{E}_i} \tag{38}$$

6.2 Exergetic efficiency

Exergetic efficiency is known as second-law efficiency, effectiveness, and rational efficiency and used to calculate the performance of the system by using the second law of thermodynamics. Exergy efficiency becomes a reliable indicator of the system's actual performance. It is necessary to analyze the fuel and product in order to determine the system's efficiency [5, 29]. The product indicates the system's desirable outcome, and the fuel expresses the resources that are utilized to produce the product. Considering the steady-state system, the fuel and product are represented in terms of exergy that are E_F and E_P, respectively. An exergy rate balance for the system is defined as follows:

$$E_F = E_P + E_D + E_L. \tag{39}$$

Here, E_D and E_L define the rate of exergy destruction and exergy loss, respectively. The efficiency ε is the ratio of the product and fuel [29]:

$$\varepsilon = \frac{E_P}{E_F} = 1 - \frac{E_D + E_L}{E_F} \tag{40}$$

Fuel, product, exergy loss, exergy destruction rate, and exergy efficiency for each component of the developed STPP (see Fig. 3) are listed in Table 4.

7 Results and discussion

The 500 kW STPP developed with the LS-3 collector is modeled in MATLAB software. This section presents and discusses the exergy analysis of the components for the newly developed system. The effect of the capacity increases on the base case and the developed system is determined. Eventually, the comparative results between the base case STPP and the developed STPP with new collector field are presented.

For the model validation, the attempt is made to compare the calculated results of the developed system in the present paper with the results of the studied system by Baghernejad and Yaghoubi [22]. They considered a base case system for Shiraz solar thermal power plant, whereas in this research tried to develop the base case system with a new collector field. Therefore, the criteria for validation of results in the developed system is based on the case study in [22]. Mass flow rate, temperature and pressure of all streams in the newly developed STPP based on their state numbers of the system (see Fig. 3) are shown in Table 5. According to the state properties represented in this table the enthalpy, entropy and exergy rates for each stream are calculated.

Energy and exergy analyses for each section of solar fields are determined by applying energy and exergy equations. Tables 6 and 7 show energy analysis results, and Tables 8 and 9 show the exergy analysis results for the collectors' fields. Comparisons of the energy and exergy analyses are shown in Tables 10 and 11. The presented results in these tables show that the lowest first and second law efficiencies in the collectors' field (Behran oil and Therminol VP-1 oil) take place at the collector–receiver subsystem. The first and second law efficiencies of the Behran oil collectors' field equal 48% and 57.05%, respectively, and in the Therminol VP-1 oil collector field equal 45.15% and 41.76%, respectively. In this subsystem, there is more energy and exergy loss than in other subsystems. In the Behran oil collectors' field, energy and exergy loss equal 51.99% and 42.94%, respectively; in the Therminol VP-1 oil collector field equal 54.84% and 58.23%, respectively.

Fuel, product, exergy destruction, and exergy efficiency for each component and the entire system in the base case (Fig. 2) studied by Baghernejad and Yaghoubi [22] and for the developed system (Fig. 3) are shown in Tables 12 and 13. Table 12 shows that the maximum exergy destruction takes place in the collectors and the auxiliary boiler with 1.46 MW and 1.113 MW. Exergy destruction and exergetic efficiency for the entire system are 6.61 MW and 7%, respectively [22]. Table 13 shows that the maximum exergy destruction occurs in the auxiliary boiler with 0.4 MW and then occurs in the Behran oil collectors' field and Therminol VP-1 oil collector's field are 0.36 MW and 0.18 MW, respectively. Exergy destruction and exergetic efficiencies for the entire developed system are about 3.1 MW and 11.97%, respectively.

In order to determine the effect of increase in the capacity of the solar hybrid power plant developed with the LS-3 collector from 500 kW to 1000 kW on the exergy performance of system, a system with 1000 kW is also run using the MATLAB software with the same code. Also, Baghernejad and Yaghoubi [23] increased the capacity of the STPP in

Table 4 Fuel, product, exergy loss, exergy destruction rate and exergy efficiency of the hybrid STPP developed with the LS-3 collector corresponding to Fig. 3

Component	Fuel	Product	Exergy loss	Exergy destruction	Exergy efficiency
Economizer	$\dot{E}_6 - \dot{E}_1$	$\dot{E}_{22} - \dot{E}_{21}$	–	$\dot{E}_6 - \dot{E}_1 - \dot{E}_{22} + \dot{E}_{21}$	$\frac{\dot{E}_{22}-\dot{E}_{21}}{\dot{E}_6-\dot{E}_1}$
Boiler	$\dot{E}_5 - \dot{E}_6$	$\dot{E}_{23} - \dot{E}_{22}$	–	$\dot{E}_5 - \dot{E}_6 - \dot{E}_{23} + \dot{E}_{22}$	$\frac{\dot{E}_{23}-\dot{E}_{22}}{\dot{E}_5-\dot{E}_6}$
Superheater 1	$\dot{E}_4 - \dot{E}_5$	$\dot{E}_{11} - \dot{E}_{23}$	–	$\dot{E}_4 - \dot{E}_5 - \dot{E}_{11} + \dot{E}_{23}$	$\frac{\dot{E}_{11}-\dot{E}_{23}}{\dot{E}_4-\dot{E}_5}$
Superheater 2	$\dot{E}_9 - \dot{E}_{10}$	$\dot{E}_{16} - \dot{E}_{11}$	–	$\dot{E}_9 - \dot{E}_{10} - \dot{E}_{16} + \dot{E}_{11}$	$\frac{\dot{E}_{16}-\dot{E}_{11}}{\dot{E}_9-\dot{E}_{10}}$
Oil heat exchanger	$\dot{E}_4 - \dot{E}_3$	$\dot{E}_{10} - \dot{E}_7$	–	$\dot{E}_4 - \dot{E}_3 - \dot{E}_{10} + \dot{E}_7$	$\frac{\dot{E}_{10}-\dot{E}_7}{\dot{E}_4-\dot{E}_3}$
Turbine	$\dot{E}_{17} - \dot{E}_{12}$	$\dot{E}_{35} = \dot{W}_{\text{turbine}}$	–	$\dot{E}_{17} - \dot{E}_{12} - \dot{W}_{\text{turbine}}$	$\frac{\dot{W}_{\text{turbine}}}{\dot{E}_{17}-\dot{E}_{12}}$
Auxiliary boiler	$\dot{E}_{21a} + \dot{E}_{33}$	$\dot{E}_{24}$	–	$\dot{E}_{21a} + \dot{E}_{33} - \dot{E}_{24}$	$\frac{\dot{E}_{24}}{\dot{E}_{21a}+\dot{E}_{33}}$
Condenser	$\dot{E}_{30} - \dot{E}_{29}$	$\dot{E}_{14} - \dot{E}_{15}$	–	$\dot{E}_{30} - \dot{E}_{29} - \dot{E}_{14} + \dot{E}_{15}$	$\frac{\dot{E}_{14}-\dot{E}_{15}}{\dot{E}_{30}-\dot{E}_{29}}$
Deaerator	$\dot{E}_{13} + \dot{E}_{18}$	$\dot{E}_{19}$	–	$\dot{E}_{13} + \dot{E}_{18} - \dot{E}_{19}$	$\frac{\dot{E}_{19}}{\dot{E}_{13}+\dot{E}_{18}}$
Oil pump Behran	$\dot{E}_{25} = \dot{W}_{\text{oilpumpbehran}}$	$\dot{E}_2 - \dot{E}_1$	–	$\dot{W}_{\text{oilpumpbehran}} - \dot{E}_2 + \dot{E}_1$	$\frac{\dot{E}_2-\dot{E}_1}{\dot{W}_{\text{oilpumpbehran}}}$
Oil pump VP-1	$\dot{E}_{27} = \dot{W}_{\text{oilpumpVP - 1}}$	$\dot{E}_8 - \dot{E}_7$	–	$\dot{W}_{\text{oilpumpVP}-1} - \dot{E}_8 + \dot{E}_7$	$\frac{\dot{E}_8-\dot{E}_7}{\dot{W}_{\text{oilpumpVP}-1}}$
Condenser pump	$\dot{E}_{31} = \dot{W}_{\text{condenserpump}}$	$\dot{E}_{18} - \dot{E}_{15}$	–	$\dot{W}_{\text{condenserpump}} - \dot{E}_{18} + \dot{E}_{15}$	$\frac{\dot{E}_{18}-\dot{E}_{15}}{\dot{W}_{\text{condenserpump}}}$
Feedwater pump	$\dot{E}_{32} = \dot{W}_{\text{feedwaterpump}}$	$\dot{E}_{20} - \dot{E}_{19}$	–	$\dot{W}_{\text{feedwaterpump}} - \dot{E}_{20} + \dot{E}_{19}$	$\frac{\dot{E}_{20}-\dot{E}_{19}}{\dot{W}_{\text{feedwaterpump}}}$
Collector	$\dot{E}_{26}$	$\dot{E}_3 - \dot{E}_2$	$(\dot{E}_L)_{\text{collector}}$	$\dot{E}_{26} - \dot{E}_3 + \dot{E}_2 - (\dot{E}_L)_{\text{collector}}$	$\frac{1-\dot{E}_{26}+\dot{E}_3-\dot{E}_2+(\dot{E}_L)_{\text{collector}}}{\dot{E}_{26}}$
LS-3 collector	$\dot{E}_{28}$	$\dot{E}_9 - \dot{E}_8$	$(\dot{E}_L)_{\text{ls - 3collector}}$	$\dot{E}_{28} - \dot{E}_9 + \dot{E}_8 - (\dot{E}_L)_{ls\text{ - 3collector}}$	$\frac{1-\dot{E}_{28}+\dot{E}_9-\dot{E}_8+(\dot{E}_L)_{\text{ls - 3collector}}}{\dot{E}_{28}}$

the base case to 1000 kW. Comparison of the performance results of the STPP developed with capacities of 500 kW and 1000 kW, and the STPP in the base case with 1000 kW capacity is carried out and listed in Table 14. The results show that increasing the capacity of the developed STPP to 1000 kW, the mass flow rate of the auxiliary boiler increases, so that it causes the fuel exergy increase from 4.08 MW to 5.5 MW, and consequently, the exergy efficiency increases from 11.97% to 18.35%, and the exergy destruction increases by 30%. The comparative results of the STPP in the base case and developed STPP with 1000 kW capacity show that exergy efficiency decreases from 18.35% to 7.4%, and the exergy destruction and the fuel exergy increase by 43.17% and 59.31% in the STPP in the form of the base case, respectively. The exergy loss is not considered in the 1000 kW STPP in the base case. These results reveal that increasing the capacity of the developed system, increases the exergy destruction and exergy efficiency. However, in the base case with 1000 kW compared with developed STPP with 500 kW, the exergy efficiency decreased, and fuel exergy and exergy destruction increased.

The comparative values of fuel consumption in the auxiliary boiler of the STPP developed with the LS-3 collector with capacities of 500 kW and 1000 kW are shown in Table 15. This table denotes that increase in the capacity to 1000 kW, increased the amount of fuel consumption in the auxiliary boiler.

Figure 4 compares the amount of exergy destruction for each component of the 500 kW hybrid STPP developed with the LS-3 collector and the 500 kW hybrid STPP in the base case [22]. The comparative results in both systems show the most exergy destruction occurs in the boiler, auxiliary boiler, and collectors' fields. The exergy destruction of an auxiliary boiler, primary collectors' field, and condenser significantly decreased in the newly developed system. This reduction value for an auxiliary boiler is due to the decrement of the fuel mass flow rate, and for the condenser is due to the decrease in mass flow rate. The exergy destruction of the superheater1 decreases slightly in the new system because of the reduction in mass flow rate. The exergy destruction of economizer and boiler value increase in the new system due to the enthalpy difference increment. The

Table 5 State properties and calculated exergy rates of the 500 kW hybrid STPP developed with the LS-3 collector corresponding to Fig. 3

State	ṁ(kg/s)	T (°C)	P (bar)	h (kJ/kg)	s (kJ/kg.K)	Ė(MW)
0 (water)	–	33	1.013	138.37	0.47	–
0 (Behran oil)	–	33	1.013	84.92	8.9	–
0 (VP-1 oil)	–	33	1.013	50.81	5.32	–
1	13.88	221	2	645.71	14.37	5.27
2	13.88	221	7.6	645.71	14.37	5.27
3	13.88	265	5.05	795.88	14.99	7.07
4	13.88	268.23	5.05	807.2	15.04	7.21
5	13.88	266.01	2.28	799.43	15.01	7.12
6	13.88	230.72	2.46	678.28	14.52	5.66
7	4.48	294	5.4	558.81	9.31	1.68
8	4.48	294	7	558.81	9.31	1.68
9	4.48	313	7	602.87	9.45	1.86
10	4.48	305.12	5.7	584.5	9.39	1.78
11	0.68	257.54	21.3	2917.1	6.54	1.77
12	1.14	64.96	0.25	2509.3	7.51	2.44
13	0.087	64.96	0.25	2509.3	7.51	0.18
14	1.05	64.96	0.25	2509.3	7.51	2.26
15	1.05	60.05	0.2	251.39	0.83	0.1
16	0.68	294	21	3007.3	6.71	1.82
17	1.14	294	21	3007.3	6.71	3.04
18	1.05	60.06	0.25	251.4	0.83	0.1
19	1.14	98.17	0.95	411.41	1.286	0.281
20	1.14	68.6	22.2	414.82	1.289	0.285
21	0.68	98.6	22.2	414.82	1.289	0.17
21a	0.45	68.6	22.2	414.82	1.289	0.11
22	0.68	217.02	21.9	929.89	2.49	0.49
23	0.68	215.1	21.1	2799.4	6.31	1.69
24	0.45	294	21	3007.3	6.71	1.21
29	8.5	33	1.01	138.37	0.47	0
30	8.5	99.96	1.01	418.93	1.3	2.15
33	0.029	33	21	641.41	11.62	1.51

Table 6 Energy analysis of the collectors' field (Behran oil)

Subsystem	Energy received (kW)	Energy delivered (kW)	Energy loss (kW)	Energy loss (%)	First law efficiency (%)
Collector	$Q_i = 3333.4$	$Q_s = 2470.1$	863.26	25.89	74.1
Receiver	$Q_s = 2470.1$	$Q_u = 1600.1$	870	35.22	64.77
Collector–receiver	$Q_i = 3333.4$	$Q_u = 1600.1$	1733.3	51.99	48

Table 7 Energy analysis of the collector field (Therminol VP-1 oil)

Subsystem	Energy received (kW)	Energy delivered (kW)	Energy loss (kW)	Energy loss (%)	First law efficiency (%)
Collector	$Q_i = 444.85$	$Q_s = 355.88$	88.97	20	80
Receiver	$Q_s = 355.88$	$Q_u = 200.88$	155	43.55	56.44
Collector–receiver	$Q_i = 444.85$	$Q_u = 200.88$	243.97	54.84	45.15

Table 8 Exergy analysis of the collectors' field (Behran oil)

Subsystem	Exergy received (kW)	Exergy delivered (kW)	Exergy loss (kW)	Exergy loss (%)	Second law efficiency (%)
Collector	$\dot{E}_i = 3156.2$	$\dot{E}_c = 2134.7$	1021.5	32.36	67.63
Receiver	$\dot{E}_c = 2134.7$	$\dot{E}_u = 1800.7$	333.96	15.64	84.35
Collector–receiver	$\dot{E}_i = 3156.2$	$\dot{E}_u = 1800.7$	1355.5	42.94	57.05

Table 9 Exergy analysis of the collector field (Therminol VP-1 oil)

Subsystem	Exergy received (kW)	Exergy delivered (kW)	Exergy loss (kW)	Exergy loss (%)	Second law efficiency (%)
Collector	$\dot{E}_i = 421.21$	$\dot{E}_c = 317.8$	104.02	24.69	75.3
Receiver	$\dot{E}_c = 317.8$	$\dot{E}_u = 175.93$	141.25	44.53	55.48
Collector–receiver	$\dot{E}_i = 421.21$	$\dot{E}_u = 175.93$	245.27	58.23	41.76

Table 10 Comparison of first and second law analysis on each subsystem of collectors' field (Behran oil)

Subsystem	Irreversibility (kW)	Energy loss (%)	Exergy loss (%)	First law efficiency (%)	Second law efficiency (%)
Collector	1021.5	25.89	32.36	74.1	67.63
Receiver	333.96	35.22	15.64	64.77	84.35
Collector–receiver	1355.55	51.99	42.94	48	57.05

Table 11 Comparison of first and second law analysis on each subsystem of collector field (Therminol VP-1 oil)

Subsystem	Irreversibility (kW)	Energy loss (%)	Exergy loss (%)	First law efficiency (%)	Second law efficiency (%)
Collector	104.02	20	24.69	80	75.3
Receiver	141.25	43.55	44.53	56.44	55.48
Collector–receiver	245.27	54.84	58.23	45.15	41.76

turbine's value exergy destruction increases because of the increase in the inlet steam's temperature from 250 °C to 294 °C. The exergy destruction of Behran oil pump increased in the developed system because of increase in the working fluid's temperature.

The performance results of the 500 kW hybrid STPP in the base case [22] and the 500 kW hybrid STPP developed with the LS-3 collector are presented in Table 16. These results indicate the exergy efficiency increases from 7% to 11.97%. Fuel exergy decreases by 42.61%. Exergy destruction decreases by 53.02% and reaches from 3.1 MW to 6.61 MW. Fuel consumption in auxiliary boiler decreases from 0.07 kg/s to 0.02 kg/s. These results illustrate that adding a Therminol VP-1 oil cycle with the LS-3 collector increases exergy efficiency, decreases the fuel consumption of the auxiliary boiler, and therefore improves total performance of the system.

Table 12 Thermodynamic Parameters of the 500 kW hybrid STPP in the base case corresponding to Fig. 2 [22]

Component	Fuel (MW)	Product (MW)	Exergy destruction (MW)	Exergetic efficiency (%)
Economizer	0.35	0.31	0.037	89.22
Boiler	1.43	1.25	0.18	86.91
Superheater	0.09	0.06	0.025	72.12
Turbine	0.523	0.5	0.023	95.61
Auxiliary boiler	3.76	2.64	1.113	70.41
Condenser	3.39	2.86	0.53	84.36
Deaerator	0.52	0.51	0.014	97.3
Oil pump Behran	0.019	0.018	0.001	91.95
Pump 1	0.0002	0.0001	0.00002	90
Pump 2	0.0119	0.0113	0.0006	95.37
Collector	3.35	1.88	1.46	56.18
System	7.11	0.5	6.61	7

Table 13 Thermodynamic Parameters of the 500 kW hybrid STPP developed with the LS-3 collector corresponding to Fig. 3

Component	Fuel (MW)	Product (MW)	Exergy destruction (MW)	Exergy loss (MW)	Exergetic efficiency (%)
Economizer	0.38	0.32	0.059	–	84.51
Boiler	1.45	1.19	0.26	–	82.08
Superheater 1	0.094	0.075	0.019	–	79.91
Superheater 2	0.073	0.058	0.015	–	78.96
Oil heat exchanger	0.138	0.102	0.035	–	74.2
Turbine	0.59	0.5	0.099	–	83.38
Auxiliary boiler	1.62	1.2	0.409	–	74.85
Condenser	2.1538	2.1534	0.0003	–	99.98
Deaerator	0.29	0.28	0.01	–	95.95
Oil pump Behran	0.0197	0.002	0.017	–	10.15
Oil pump VP-1	0.0013	0.0002	0.0011	–	15.38
Condenser pump	0.000008	0.000005	0.000003	–	63.03
Feedwater pump	0.0039	0.0038	0.00012	–	96.9
Collector	2.13	1.8	0.034	0.33	84.35
LS-3 collector	0.31	0.17	0.041	0.14	55.47
System	4.08	0.5	3.1	0.47	11.97

Table 14 Comparative results of the hybrid STPP developed with LS-3 collector with capacities of 500 kW and 1000 kW

Properties	Developed hybrid STPP with LS-3 collector (500 kW)	Developed hybrid STPP with LS-3 collector (1000 kW)	Hybrid STPP in the form of the base case (1000 kW) [22]
Fuel exergy (MW)	4.08	5.5	13.52
Product exergy (MW)	0.5	1	1
Exergy destruction (MW)	3.1	4.03	5.77
Number of collectors	48	48	48
Number of LS-3 collectors	1	1	0
Exergy efficiency (%)	11.97	18.35	7.4

Table 15 Comparative fuel consumption in the auxiliary boiler of hybrid STPP developed with the LS-3 collector with capacities of 500 kW and 1000 kW

	Developed hybrid STPP with LS-3 collector (500 kW)	Developed hybrid STPP with LS-3 collector (1000 kW)
Fuel consumption in auxiliary boiler (kg/s)	0.02	0.05

8 Conclusions and recommendations

The purpose of the present study is to do energy and exergy analyses of the 500 kW hybrid STPP developed with the LS-3 collector and to compare the results with a 500 kW hybrid STPP in the base case. The STPP is investigated in the view of the energy and exergy analyses in order to improve the total performance of system. The results obtained from the exergy analysis of the hybrid STPP show:

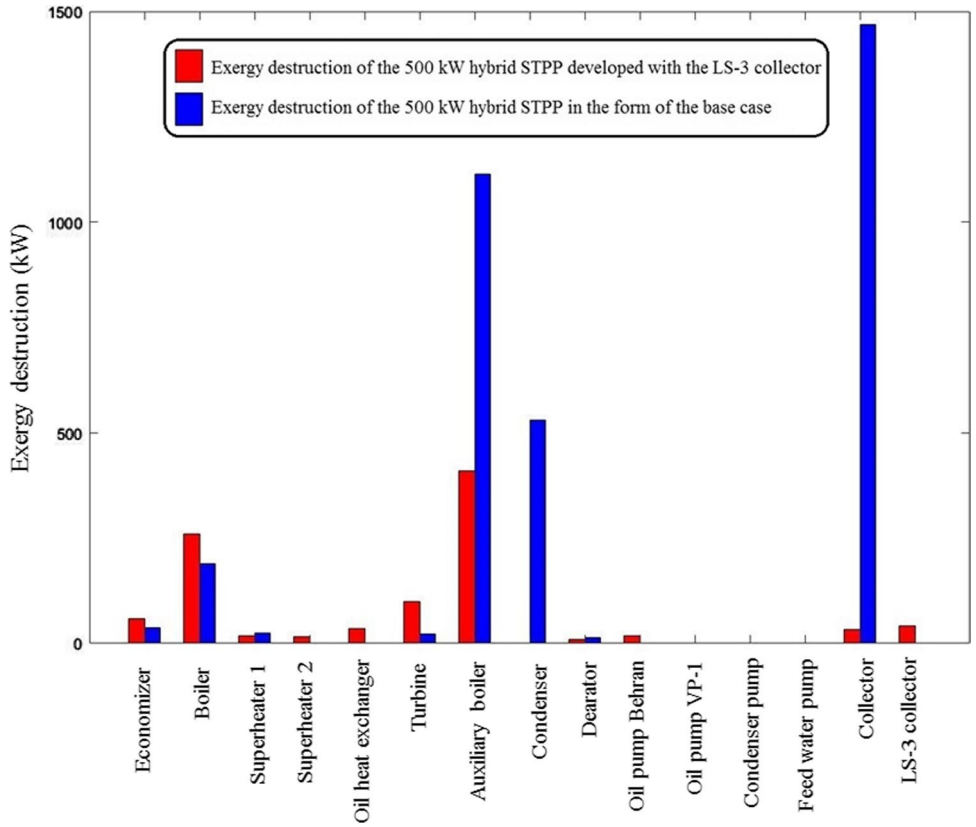

Fig. 4 Comparative exergy destruction of the 500 kW hybrid STPP developed with the LS-3 collector and the 500 kW hybrid STPP in the form of the base case [22]

Table 16 Comparative results of the 500 kW hybrid STPP in the form of the base case [22] and the 500 kW hybrid STPP developed with the LS-3 collector

Properties	Hybrid STPP in the form of the base case (500 kW) [22]	Developed hybrid STPP with the LS-3 collector (500 kW)
Fuel exergy (MW)	7.11	4.08
Product exergy (MW)	0.5	0.5
Exergy destruction (MW)	6.61	3.1
Exergy efficiency (%)	7	11.97
Fuel consumption in auxiliary boiler (kg/s)	0.07	0.02

- In the solar fields, the lowest first and second law efficiency in the collectors' fields (Behran oil and Therminol VP-1 oil) occurs at the collector–receiver subsystem. In this subsystem, in the Therminol VP-1 oil collector field, there is more energy and exergy loss than other subsystems.
- The main source of exergy destruction in the developed STTP system is the auxiliary boiler equal 0.4 MW and then in the solar collectors fields equal 0.54 MW due to the high energy loss. Exergy destruction and exergetic efficiency for the entire system equal 3.1 MW and 11.97%, respectively.
- Increasing the capacity from 500 kW to 1000 kW, increases the exergy efficiency, exergy destruction, and fuel exergy in the developed STPP. While in the base case 500 kW STPP, the exergy efficiency decreases, and fuel exergy and exergy destruction increase. In addition, comparison of the results for these two systems with 1000 kW capacity shows that exergy efficiency increases, and exergy destruction and fuel exergy decrease in the developed STPP.
- Systems' comparative results show exergy efficiency increases from 7% in the base case to 11.97% in the developed case. Exergy destruction, fuel exergy, and fuel consumption in an auxiliary boiler are decreased by 53.02%, 42.61%, 60.27%, respectively, in the developed STPP system.

It is recommended that more research be done in the following areas:

- To apply thermodynamic optimization to increase exergy efficiency. Maximizing exergy efficiency means minimizing exergy destruction.
- To perform exergoeconomic analysis and thermoeconomic optimization to minimize the cost of exergy destruction.

Authors' contribution AB presented, designed and analyzed the study. EJ performed the exergy analysis and organized the results and wrote the first draft of the manuscript. AB and EJ contributed to manuscript revision, and read and approved the submitted version.

Funding The authors have no financial or proprietary interests in any material discussed in this article.

Declarations

Conflict of interest There is no conflict of interest for this manuscript.

Availability of data and material The data that support the findings of this study are available from the corresponding author, upon reasonable request.

Code availability All code for data analysis associated with the current submission is available.

References

1. Chattopadhyay S, Ghosh S (2020) Thermo - economic assessment of a hybrid tri - generation system making simultaneous use of biomass and solar energy. J Brazilian Soc Mech Sci Eng. https://doi.org/10.1007/s40430-020-02641-7
2. Reis C, Carlos P, Keutenedjian E (2020) Comparing the thermodynamic performance of organic Rankine and Kalina cycles in solar energy systems. J Brazilian Soc Mech Sci Eng. https://doi.org/10.1007/s40430-020-02682-y
3. Islam MT, Huda N, Abdullah AB, Saidur R (2018) A comprehensive review of state-of-the-art concentrating solar power (CSP) technologies: Current status and research trends. Renew Sustain Energy Rev 91:987–1018. https://doi.org/10.1016/j.rser.2018.04.097
4. Palenzuela P, Alarcón-Padilla DC, Zaragoza G (2015) Concentrating solar power and desalination plants: engineering and economics of coupling multi-effect distillation and solar plants. Springer International Publishing
5. Dincer I, Rosen MA, Ahmadi P (2017) Optimization of energy systems. Wiley
6. Dincer I (2018) Comprehensive energy systems. Elsevier
7. Cavalcanti EJC, Azevedo JLB (2021) Energy, exergy and exergoenvironmental (3E) analyses of power plant integrated with heliostats solar field. J Brazilian Soc Mech Sci Eng 43:1–13. https://doi.org/10.1007/s40430-021-02893-x
8. Kaushik S, Misra R, Singh N (2000) Second law analysis of a solar thermal power system. Int J Sol Energy 20:239–253. https://doi.org/10.1080/01425910008914358
9. Singh N, Kaushik SC, Misra RD (2000) Exergetic analysis of a solar thermal power system. Renew Energy 19:135–143. https://doi.org/10.1016/s0960-1481(99)00027-0
10. Wu JQ, Zhu DF, Wang H, Zhu Y (2013) Exergetic analysis of a solar thermal power plant. Adv Mater Res 724–725:156–162. https://doi.org/10.4028/www.scientific.net/AMR.724-725.156
11. Noorpoor AR, Hamedi D, Hashemian N (2017) Optimization of parabolic trough solar collectors integrated with two stage Rankine cycle. J Sol Energy Res 2:61–66
12. Vakilabadi MA, Bidi M, Najafi AF, Ahmadi MH (2019) Exergy analysis of a hybrid solar-fossil fuel power plant. Energy Sci Eng 7:146–161. https://doi.org/10.1002/ese3.265
13. Al-Sulaiman FA (2014) Exergy analysis of parabolic trough solar collectors integrated with combined steam and organic Rankine cycles. Energy Convers Manag 77:441–449. https://doi.org/10.1016/j.enconman.2013.10.013
14. Kerme ED, Orfi J (2015) EXERGY-BASED THERMODYNAMIC ANALYSIS OF SOLAR DRIVEN ORGANIC * Corresponding Author : Esa Dube Kerme. J Therm Eng 1:192–202
15. Singh H, Mishra RS (2018) Performance evaluation of the supercritical organic rankine cycle (SORC) integrated with large scale solar parabolic trough collector (SPTC) system: an exergy energy analysis. Environ Prog Sustain Energy 37:891–899. https://doi.org/10.1002/ep.12735
16. Habibi H, Zoghi M, Chitsaz A et al (2019) Thermo-economic performance comparison of two configurations of combined steam and organic Rankine cycle with steam Rankine cycle driven by Al_2O_3-therminol VP-1 based PTSC. Sol Energy 180:116–132. https://doi.org/10.1016/j.solener.2019.01.011
17. Mohammadi A, Ahmadi MH, Bidi M et al (2018) Exergy and economic analyses of replacing feedwater heaters in a Rankine cycle with parabolic trough collectors. Energy Rep 4:243–251. https://doi.org/10.1016/j.egyr.2018.03.001
18. Akbari Vakilabadi M, Bidi M, Najafi AF (2018) Energy, Exergy analysis and optimization of solar thermal power plant with

adding heat and water recovery system. Energy Convers Manag 171:1639–1650. https://doi.org/10.1016/j.enconman.2018.06.094
19. Alrobaian AA (2020) Combination of passive and active enhancement methods for higher efficiency of waste-fired plants; flue gas and solar thermal processing. J Brazilian Soc Mech Sci Eng 42:1–13. https://doi.org/10.1007/s40430-020-02692-w
20. Yaghoubi M, Azizian K, Kenary A (2003) Simulation of Shiraz solar power plant for optimal assessment. Renew Energy 28:1985–1998. https://doi.org/10.1016/S0960-1481(03)00069-7
21. Azizian K, Yaghoubi M, Hesami R, Mirhadi S (2010) Shiraz pilot solar thermal power plant design, construction, installation and commissioning procedure. In: 7th International Conference on Heat Transfer, Fluid Mechanics and Thermodynamics. pp 1–6
22. Baghernejad A, Yaghoubi M (2013) Thermoeconomic methodology for analysis and optimization of a hybrid solar thermal power plant. Int J Green Energy 10:588–609. https://doi.org/10.1080/15435075.2012.706672
23. Azizian K, Yaghoubi M, Hesami R, Kanan P (2011) Design analysis for expansion of shiraz solar power plant to 500 kW power generation capacity. proc world renew energy Congr – Sweden, 8–13 May, 2011. Linköping, Sweden 57:3897–3904. https://doi.org/10.3384/ecp110573897
24. Niknia I, Yaghoubi M (2012) Transient simulation for developing a combined solar thermal power plant. Appl Therm Eng 37:196–207. https://doi.org/10.1016/j.applthermaleng.2011.11.016
25. Baghernejad A, Yaghoubi M (2010) Exergy analysis of an integrated solar combined cycle system. Renew Energy 35:2157–2164. https://doi.org/10.1016/j.renene.2010.02.021
26. Yaghoubi M, Zarrini S, Mirhadi S (2011) Optimum integration of a large size collector to a solar thermal power plant. Proc World Renew Energy Congr – Sweden, 8–13 May, 2011. Linköping, Sweden 57:3859–3865. https://doi.org/10.3384/ecp110573859
27. Baghernejad A, Yaghoubi M (2011) Exergoeconomic analysis and optimization of an Integrated Solar Combined Cycle System (ISCCS) using genetic algorithm. Energy Convers Manag 52:2193–2203. https://doi.org/10.1016/j.enconman.2010.12.019
28. Enteria N, Akbarzadeh A (2013) Solar energy sciences and engineering applications, 1st edn. CRC Press
29. Bejan A, Tsatsaronis G, Moran MJ (1995) Thermal design and optimization. Wiley